*Desalination and Water Treatment*
www.deswater.com

doi: 10.5004/dwt.2021.26563

212 (2021) 164–172
February

# Ultrasonic-assisted adsorption of propyl paraben on ultrasonically synthesized $TiO_2$ nanoparticles loaded on activated carbon: optimization, kinetic and equilibrium studies

Maryam Pargari, Farzaneh Marahel*, Bijan Mombini Godajdar

*Department of Chemistry, Omidiyeh Branch, Islamic Azad University, Omidiyeh, Iran, emails: farzane.marahel.fm@gmail.com (F. Marahel), maryampargari@gmail.com (M. Pargari), bmombini@gmail.com (B.M. Godajdar)*

Received 14 December 2019; Accepted 12 September 2020

**ABSTRACT**

In deleting dyes from aqueous solutions, the applicability of $TiO_2$ nanoparticles loaded on activated carbon ($TiO_2$ NPs–AC) synthesis has gained attention. The focal attention of this paper was directed at the development of an operative methodology to procure the best possible removal conditions through the instrumentality of ultrasonic to maximize the deletion of propyl paraben dye with the lowest deleting errors. Through the use of response surface methodology (RSM), propyl paraben dye could load up onto $TiO_2$ nanoparticles loaded on activated carbon ($TiO_2$ NPs–AC) in aqueous solution in no time. Certain techniques in particular Fourier transform infrared spectroscopy, X-ray diffraction and scanning electron microscopy were employed to characterize this unique material. Also, the impacts of variables including initial propyl paraben concentration ($X_1$), pH ($X_2$), adsorbent dosage ($X_3$), sonication time ($X_4$) came under scrutiny using central composite design (CCD) under RSM. The influences of variables such as initial propyl paraben concentration ($X_1$), pH ($X_2$), adsorbent dosage ($X_3$), sonication time ($X_4$) investigated by CCD under response surface methodology. The process was empirically modeled to reveal the significant variables and their possible interactions. The optimization conditions were set as: 3 min, 4.0, 0.027 g, 12 mg $L^{-1}$ for ultrasound time, pH, adsorbent mass, propyl paraben concentration, respectively. Finally, it was found that the equilibrium and kinetics of the adsorption process follow the Langmuir isotherm and pseudo-second-order kinetic model, respectively. The adsorbent was proved to be recyclable for more than once. Since almost 99.5% of propyl paraben was deleted with ideal adsorption capacities ($Q_{max}$) was found to be 120 mg $g^{-1}$ for propyl paraben at optimum conditions. Therefore not only the short-time adsorption process was considered an advantage but also other advantages in using $TiO_2$ nanoparticles loaded on activated carbon ($TiO_2$ NPs–AC) such as being recyclable, safe and cost-efficient made it a promising and powerful material for the wastewater treatment.

*Keywords:* Adsorption capacities; Propyl paraben; Isotherm; $TiO_2$ nanoparticles loaded on activated carbon; Response surface methodology

## 1. Introduction

Parabens are esters of p-hydroxybenzoic acid and are used as preservatives and as antimicrobials in many personal care products (PCPs), as well as in pharmaceutical preparations [1], food commodities, beverages and industrial products. Parabens are found in sunscreen creams, toothpastes, cosmetics, glues, fats and oils. Their broad use in consumer products [2] is due to their antibacterial and antifungal [3] properties as well as their favorable human safety profile. A potential relationship has been found between daily use of parabens containing PCPs and breast cancer [4] as well as melanoma in younger people [5]. Some

* Corresponding author.

published studies have also reported that the high concentrations of parabens are able to cause male reproductive disorders [6]. Due to all the above applications of parabens, they routed to wastewater treatment plants. Parabens are removed in a considerable extension during some wastewater treatment technologies [7]. Nevertheless, they have been identified in river water samples at the low ng $L^{-1}$ level [8]. Moreover, parabens have been detected in soil and sediment samples [9,10]. The fate of the pollutants in the environment and especially in the water is controlled by a series of physical, chemical and biological processes. Ultrasound irradiation is well known to accelerate chemical process due to the phenomenon of acoustic cavitation, that is, the formation, growth and collapse of micrometrical bubbles, formed by the propagation of a pressure wave through a liquid [11,12]. Ultrasound, and its secondary effect, cavitation (nucleation, growth and transient collapse of tiny gas bubbles) improve the mass transfer through convective pathway that is emerged from physical phenomena such as micro-streaming, micro-turbulence, acoustic (or shock) waves and micro jets without significant change in equilibrium characteristics of the adsorption/desorption system [13–15]. Shock waves have the potential of creating microscopic turbulence within interfacial films surrounding nearby solid particles [16]. Acoustic streaming induced by the sonic wave is the movement of the liquid, which can be considered to be the conversion of sound to the kinetic energy [17]. Ultrasound has been proven to be a very useful tool in intensifying the mass transfer process and breaking the affinity between adsorbate and adsorbent [18–20].

Adsorption is one of the best and simple techniques for the removal of toxic and noxious impurities in comparison with other conventional protocols such as chemical coagulation, ion exchange, electrolysis, biological treatments and is related to advantages viz. lower waste, higher efficiency and simpler and milder operational conditions. Adsorption techniques also have more efficiency in the removal of pollutants, which are highly stable in biological degradation process through economically feasible mild pathways [21]. Hence, it has been extensively used for removal of different chemicals from aqueous solutions of these methods, nanomaterials-based adsorbents are highly recommended for dyes pollutants removal [22].

In improving removal efficiency, detecting novel adsorbent materials has always been the most prominent issue in adsorption technique [23]. Nanotechnology as an inviting area of research principally focuses on developing nanoparticles with varied sizes, chemical compositions, shapes, dispersity and possible application that can serve for the benefit of mankind [24]. The physical and chemical characteristics of the adsorbent are effective to a great extent on the efficacious applicability of an adsorption process. Amongst these characteristics, having great adsorption capacity and being renewable, available and affordable are mentionable. Nowadays, a lot has been done by testing different potential adsorbents to find out whether they are successful in removing specific organics from water samples. From this perspective, numerous studies have been done on magnetic nanoparticles as unique adsorbents with high adsorption capacity, large surface area and small diffusion resistance. They have been employed for separation of chemical species such as environmental pollutants, metals, dyes and gases [25]. Currently, a few studies by some research groups have revealed that sonication plays a key role in diminishing the adsorption time and boosting the contact of samples with the adsorbent, which can lead to more effective mass transfer to the porosity of the adsorbent, and internal and external area of it [26,27].

In this current article, the synthesis of a unique adsorbent named $TiO_2$ nanoparticles-loaded on AC ($TiO_2$ NPs–AC) was easily carried out and subsequently through the instrumentality of scanning electron microscopy (SEM), Fourier transform infrared spectroscopy (FTIR) and X-ray diffraction (XRD) analysis, they were characterized. In propyl paraben elimination process, with the help of central composite design (CCD) under response surface methodology (RSM), the selection and optimization of the ensuing experimental conditions were performed: (1) pH, (2) contact time, (3) initial propyl paraben concentration, (4) adsorbent dosage and (5) the propyl paraben dye removal percentage. This fact that the adsorption of propyl paraben follows the pseudo-second-order rate equation was clearly proven. Furthermore, it was demonstrated that the Langmuir model could undoubtedly be used for the equilibrium data explanation. The pseudo-second-order model was in control of the kinetics of adsorption process which was confirmed through the analysis of kinetic models (both pseudo-first-order, pseudo-second-order diffusion models). The capability of $TiO_2$ nanoparticles loaded on AC ($TiO_2$ NPs–AC) in elimination of propyl paraben dye from wastewater was demonstrated by evidences [28].

## 2. Experimental setup

### 2.1. Reagents and instruments

Propyl paraben, activated carbon, sodium hydroxide, hydrochloric acid, ethanol and titanium tetrachloride were supplied by Merck (Darmstadt, Germany). The morphology of samples was studied by SEM (KYKY-EM 3200, Hitachi Company, China) under an acceleration voltage of 26 kV). The FTIR spectra of compounds were recorded on a JASCO-680 instrument (JASCO Company, Tokyo, Japan) over the range of 400–4,000 $cm^{-1}$ using KBr pellet with samples to KBr ratio of 1:100. XRD pattern was recorded by an automated Philips X'Pert X-ray diffractometer from Netherlands. An ultrasonic bath with heating system (Tecno-Gaz Company SPA Ultrasonic System, Italy) at frequency of 40 kHz and power of 130 W was used for the ultrasound-assisted adsorption. The pH/ion meter (model-728, Metrohm Company, Switzerland) was used for the pH measurements. propyl paraben concentrations were determined using Jasco UV-Vis spectrophotometer model V-530 (Jasco Company, Japan).

### 2.2. Preparation of $TiO_2$ NPs–AC

Titanium dioxide nanoparticles were synthesized by the sol–gel process at room temperature directly from titanium tetrachloride and ethanol. 2 mL of titanium tetrachloride was added in 20 mL of dry ethanol drop wise under stirring.

Obtained solution was maintained at room temperature for 36 h to obtain a homogeneous gel which was then dried at 80°C and calcined at 500°C for 2 h. The titanium dioxide ($TiO_2$) loaded onto the AC with a weight ratio of 1:10 in the following manner: AC was thoroughly dispersed in 250 mL of ethanol under sonication for 1 h, Then 0.2 g of titanium NPs were added to ethanolic mixture. The suspension was sonicated for 1 h and stirred for 20 h at 400 rpm. $TiO_2$ NPs–AC was filtrated by centrifugation and dried for 18 h at 80°C.

### 2.3. Adsorption experiments

According to experimental runs in the CCD, the pH of various solutions with different concentration of propyl paraben was adjusted using concentrated HCl and/or NaOH into a 50 mL Erlenmeyer flask while mixed thoroughly with specific amounts of adsorbent. The experiments were performed at room temperature during predetermined sonication time in an ultrasonic bath. At the end of the adsorption process, the sample solution was immediately centrifuged and the supernatant containing residue was analyzed by a double-beam UV-Vis spectrophotometer (Jasco, Model UV-vis V-530, Japan) was the propyl paraben dye the concentrations in the solution were measured at 670 nm. The calculation of the quantity of adsorbed propyl paraben dye at equilibrium ($q_e$ (mg $g^{-1}$)) was done applying the ensuing equation:

$$\%A = \frac{C_0 - C_e}{C_t} \times 100 \quad (1)$$

where $C_0$ (mg $L^{-1}$) in the above equation is the concentration of target at initial time $t$ and $C_t$ (mg $L^{-1}$) is that after time $t$.

$$q_e = \frac{\left(C_0 - C_e\right)V}{W} \quad (2)$$

where $C_0$ (mg $L^{-1}$) is the initial propyl paraben dye concentration and $C_e$ (mg $L^{-1}$) refers to equilibrium propyl paraben dye concentration in aqueous solution. The solution volume and the adsorbent mass are shown by $V$ (L) and $W$ (g), respectively. The evaluation of the thermodynamic properties of the adsorption process was performed by adding 0.027 g of $TiO_2$ NPs–AC into 100 mL initial propyl paraben dye concentration ranging from 5 to 25 mg $L^{-1}$ in each experiment. At pH of 4.0 for propyl paraben dye, within 3 min and at 25°C, each solution was shaken uninterruptedly. The propyl paraben dye concentration was estimated after the solution equilibrium and the desorption outcomes were obtained [29,30].

### 2.4. Statistical analysis

CCD as most applicable type of RSM was applied for modeling and the optimization of effects of concentration of propyl paraben ($X_1$), pH ($X_2$), amount of adsorbent ($X_3$) and contact time ($X_4$) on the ultrasonic-assisted adsorption of propyl paraben by $TiO_2$ NPs–AC. Four independent variables were set at five levels at which the $R$% of propyl paraben as response was determined and shown in Tables 1 and 2. Analysis of variance (ANOVA) was performed to evaluate the important and effective terms for modeling the response based on $F$-test and $p$-values [31,32].

### 2.5. Desirability function

Desirability function (DF) creates a function for each individual response leading to final output of global function ($D$), maximum value of which supports the achievement of optimum value [33]. The principle and application of DF for the best prediction of real behavior of adsorption system was pointed out previously [34]. The desirability profiles indicate the predicted levels of variables, which produce the most desirable responses.

## 3. Results and discussion

### 3.1. Characterization of adsorbent $TiO_2$ nanoparticles loaded on activated carbon

#### 3.1.1. FTIR analysis

The FTIR spectra of $TiO_2$ NPs–AC are shown in Fig. 1; in the range 500–3,500 $cm^{-1}$ corresponding to the various vibrations involved. The absorption band at 533 $cm^{-1}$ may be attributed to angular deformation and Ti–O stretching modes of $TiO_2$ NPs. In the range of 1,500–3,500 $cm^{-1}$, water has three dominant peaks. One peak appears at ~3,414 $cm^{-1}$, which corresponds to the symmetric and asymmetric stretching. The next appears at 2,382 $cm^{-1}$, which is a combination band due to the bending and vibrational modes of H–O–H and the last one appears at 1,632 $cm^{-1}$, which is due to H–O–H bending. Absorption peak at 1,733 $cm^{-1}$ corresponding to the stretching vibration of carbonyl groups. The broad peaks at 1,029 $cm^{-1}$ could be assigned to C–O stretching from phenolic, alcoholic, etheric groups and to C–C bonds. Absorption band at 872 $cm^{-1}$ is attributed to the lattice O–H bending vibration [35].

Table 1
Process variables and their level for the propyl paraben adsorption by central composite design

| Factors | Levels | | | Star point $\alpha$ = 2.0 | |
|---|---|---|---|---|---|
| | Low (–1) | Central (0) | High (+1) | $-\alpha$ | $+\alpha$ |
| ($X_1$) PP concentration (mg $L^{-1}$) | 10 | 15 | 20 | 5 | 25 |
| ($X_2$) pH | 5.0 | 6.0 | 7.0 | 4.0 | 8.0 |
| ($X_3$) Adsorbent mass (g) | 0.0150 | 0.0225 | 0.0300 | 0.005 | 0.045 |
| ($X_4$) Sonication time (min) | 3.0 | 4.0 | 5.0 | 2.0 | 6.0 |

Table 2
Design matrix and the response

| Run | $X_1$ | $X_2$ | $X_3$ | $X_4$ | $R$% propyl paraben |
|---|---|---|---|---|---|
| 1 | 20 | 8 | 0.03 | 5 | 100 |
| 2 | 30 | 4 | 0.02 | 5 | 98.36 |
| 3 | 25 | 6 | 0.015 | 4 | 97.84 |
| 4 | 25 | 6 | 0.025 | 2 | 99.76 |
| 5 | 20 | 4 | 0.03 | 5 | 100 |
| 6 | 30 | 8 | 0.02 | 3 | 97 |
| 7 | 25 | 6 | 0.025 | 4 | 99.52 |
| 8 | 25 | 6 | 0.025 | 6 | 100 |
| 9 | 25 | 6 | 0.025 | 4 | 100 |
| 10 | 25 | 2 | 0.025 | 4 | 100 |
| 11 | 20 | 4 | 0.02 | 3 | 100 |
| 12 | 25 | 6 | 0.025 | 4 | 100 |
| 13 | 30 | 4 | 0.03 | 5 | 100 |
| 14 | 20 | 8 | 0.02 | 3 | 99 |
| 15 | 20 | 4 | 0.03 | 3 | 100 |
| 16 | 20 | 4 | 0.02 | 5 | 99.58 |
| 17 | 25 | 6 | 0.025 | 4 | 99.19 |
| 18 | 30 | 4 | 0.03 | 3 | 100 |
| 19 | 15 | 6 | 0.025 | 4 | 100 |
| 20 | 20 | 8 | 0.02 | 5 | 100 |
| 21 | 25 | 6 | 0.025 | 4 | 99 |
| 22 | 30 | 8 | 0.03 | 3 | 98 |
| 23 | 25 | 6 | 0.025 | 4 | 98.65 |
| 24 | 30 | 4 | 0.02 | 3 | 98.5 |
| 25 | 35 | 6 | 0.025 | 4 | 97 |
| 26 | 30 | 8 | 0.02 | 5 | 97.64 |
| 27 | 20 | 8 | 0.03 | 3 | 100 |
| 28 | 25 | 6 | 0.035 | 4 | 100 |
| 29 | 30 | 8 | 0.03 | 5 | 99.21 |
| 30 | 25 | 10 | 0.025 | 4 | 98.39 |

#### 3.1.2. XRD analysis

The XRD pattern of the $TiO_2$ nanoparticles loaded on activated carbon ($TiO_2$ NPs–AC) is shown in Fig. 2. The synthesized nanopowders are found to be polycrystalline in nature. All detectable peaks corresponding to (101), (110), (400), (200), (105), (211), (204), (220) and (301) planes belong to the $TiO_2$ nanoparticles loaded on activated carbon ($TiO_2$ NPs–AC) (JCPDS no. 78–1901) [36].

Surface morphology of $TiO_2$ nanoparticles loaded on activated carbon ($TiO_2$ NPs–AC), depicted to be homogeneous, smooth, regular and almost equal size distribution as individual particles as well as aggregates.

The graph in Fig. 3 shows the morphological features and particle size distribution of the $TiO_2$ nanoparticles loaded on activated carbon ($TiO_2$ NPs–AC) using SEM micrograph. It has been seen that the particles were mostly spherical with a various size distribution as they form agglomerates. From the particle size distribution, we obtain the average particle size in the range of 30–45 nm very close to those determined by XRD analysis [37].

### 3.2. Analysis of central composite design

ANOVA was performed to obtain information on the most important variables and their possible interactions (Table 3). Accordingly to the model, $F$-value of 12.07 and very small $p$-values (<0.0001) for most terms indicated the high suitability and applicability of the model for the prediction of propyl paraben removal within 95% confidence level. The "Lack of Fit $F$-value" of 0.23 and the corresponding $p$-value implied the significance of this model for the prediction of experimental data. The values of the determination coefficient $R^2$ (0.91849) and the adjusted $R^2$ (0.91) also confirm the applicability of the model for predicting the removal percentage of propyl paraben. Therefore, the following semi-empirical expression applies to model the removal percentage ($R$%) of propyl paraben:

$$\begin{aligned} R\%_{\text{propyl paraben}} = {} & 99.393 - 0.66125X_1 - 0.36708X_2 + 0.47708X_3 \\ & + 0.11542X_4 - 0.27687X_1X_2 + 0.26813X_1X_3 \\ & + 0.070625X_1X_4 + 0.00062500X_2X_3 \\ & + 0.21313X_2X_4 + 0.0081250X_3X_4 - 0.20969X_1^2 \\ & - 0.035937X_2^2 - 0.10469X_3^2 + 0.13531X_4^2 \end{aligned} \quad (1)$$

To make another convenient assessment on the applicability of the model, the predicted and observed values of the removal percentage of propyl paraben on $TiO_2$ NPs–AC were compared (Fig. 4), which showed a good fit.

The profile for predicted values and desirability option (not shown) was used to optimize the adsorption process. Profiling the desirability of response involves specifying the DF for $R$% (PP) as dependent variable by assigning the predicted $R$% PP values. The scale in the range of 0.0 (undesirable) to 1.0 (very desirable) is used to obtain a comprehensive function that should be maximized according to the efficient selection and optimization of designed variables. The CCD design matrix results (Table 3) show the maximum (100%) and minimum (65.0%) of $R$% (PP). Regarding this range, the optimum condition, at which the maximum response is achieved, was obtained. From these calculations and desirability score of 1.0, maximum recovery of 99.83% was obtained at optimum conditions. 3 min, 4, 0.027 g, 12 mg $L^{-1}$ for the sonication time, pH, adsorbent mass, propyl paraben concentration, respectively. At this condition, $R$% (PP) was predicted to be 99.8% with desirability of 0.99. The validity of the predicted response at optimum condition was checked by performing three experiments at similar condition. In average, the experimental response was obtained to be 99.5%, which is in excellent consistency with the predicted value.

### 3.3. Response surface methodology

The 3D response surface plots were used to illustrate the combined effects and identify the major interactions between variables on $R$% of understudy propyl paraben. In this work, typically four 3D response surface plots are shown in Fig. 4, that is, the removal percentage changes vs. the adsorbent dosage. The positive increase in the propyl paraben

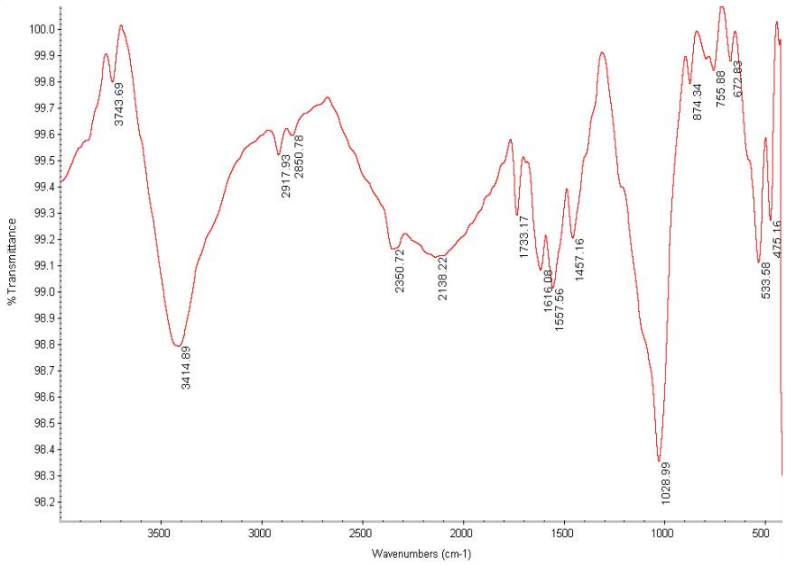


Fig. 1. FTIR transmittance spectrum of the prepared $TiO_2$ NPs–AC.

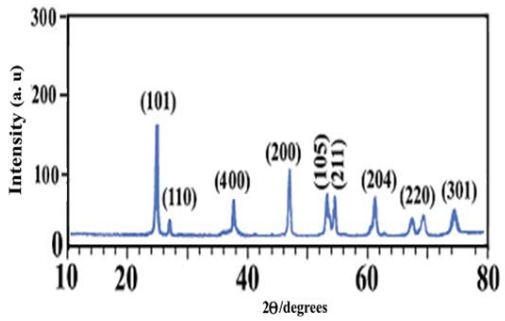


Fig. 2. XRD patterns of $TiO_2$ nanoparticles loaded on activated carbon ($TiO_2$ NPs–AC).

removal percentage with increase in adsorbent mass is seen. Significant diminish in removal percentage at lower amount of $TiO_2$ NPs–AC is attributed to higher ratio of propyl paraben molecules to the vacant sites of the adsorbent. The effect of contact time on the propyl paraben removal percentage is shown in Fig. 4c. As seen, the maximum propyl paraben adsorption could be achieved in short sonication time that strongly supports high contribution of ultrasound power in mass transfer and thus the higher efficiency for the adsorption of propyl paraben. In other words, the application of ultrasound simultaneously increases the diffusion coefficient of propyl paraben and mass transfer of aggregate to the surface area and vacant sites of adsorbent.

### 3.4. Adsorption equilibrium

The experimental adsorption equilibrium data were evaluated for studying the mechanism of propyl paraben adsorption onto $TiO_2$ NPs–AC using different models such as Langmuir, Freundlich, Temkin, Dubinin–Radushkevich isotherms [38–40] in their conventional linear form. Subsequently, their corresponding constants were evaluated from the slopes and intercepts of respective lines (Table 4). These models were applied at optimal dosages of adsorbent while other variables were kept at optimal condition (Table 4). Fitting the experimental data to these isotherm models and considering the higher values of correlation coefficients ($R^2$ = 0.999) for propyl paraben, it was concluded that the Langmuir isotherm is the best model to explain the propyl paraben adsorption onto $TiO_2$ NPs–AC, which quantitatively describes the formation of a monolayer of adsorbate on the outer surface of the $TiO_2$ NPs–AC. It also shows the equilibrium distribution of propyl paraben between the solid and liquid phases.

### 3.5. Adsorption kinetics

The kinetics of reactions in adsorption process is strongly influenced by several parameters related to the state of the solid and to the physico-chemical conditions under which sorption is occurred. To investigate the sorption processes of propyl paraben onto the adsorbent, different kinetic models such as pseudo-first-order, pseudo-second-order, Elovich and intraparticle diffusion models were studied [38,39,41]. The various parameters were calculated from the plots of the kinetic model equations (Table 5). Among these models, the criterion for their applicability is based on the judgment on the respective correlation coefficient ($R^2$) and agreement between experimental and calculated values of $q_e$. The high values of $R^2$ (0.999) and good agreement between two $q_e$ values indicate that this adsorption system follows pseudo-second-order kinetic model, which was developed based on the assumption that limiting step may be a chemisorption process.

## 4. Conclusion

A thorough investigation was performed on the effectiveness of synthesized titanium dioxide nanoparticles loaded on activated carbon as an adsorbent for the deletion of propyl paraben dye from aqueous solutions. Response

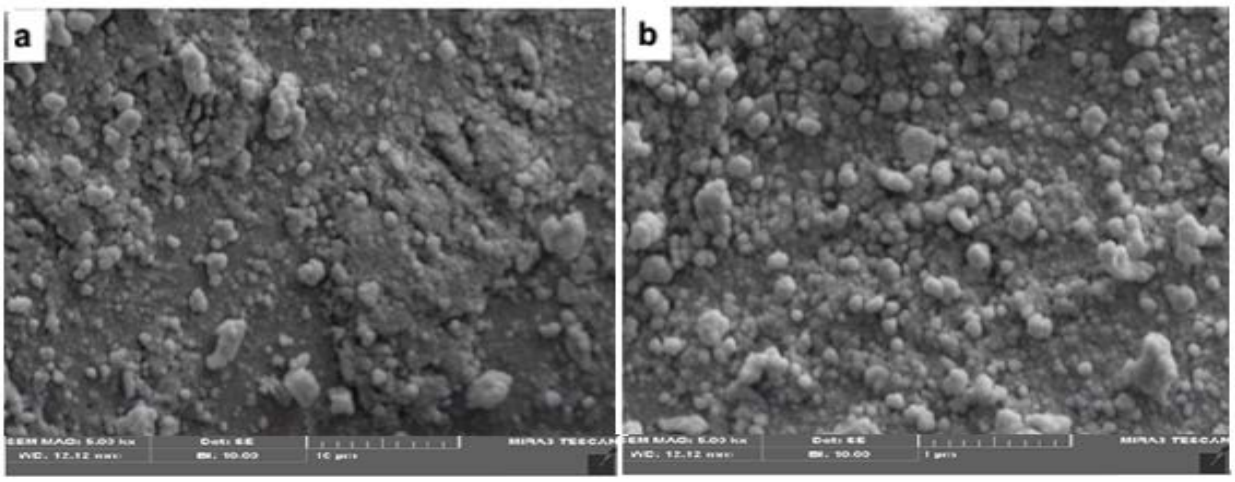


Fig. 3. FE-SEM (a and b) images of surface modified $TiO_2$ nanoparticles.

Table 3
Results of ANOVA for the response surface quadratic model

| Source of variation | Df | Propyl paraben | | | |
|---|---|---|---|---|---|
| | | Sum of square | Mean square | *F*-value | *p*-value |
| Model | 14 | 24.932 | 1.7808 | 12.073 | <0.0001 |
| $X_1$ | 1 | 10.494 | 10.494 | 71.145 | <0.0001 |
| $X_2$ | 1 | 3.2340 | 3.2340 | 21.925 | 0.00029477 |
| $X_3$ | 1 | 5.4626 | 5.4626 | 37.034 | <0.0001 |
| $X_4$ | 1 | 0.31970 | 0.31970 | 2.1674 | 0.16163 |
| $X_1X_2$ | 1 | 1.2266 | 1.2266 | 7.7982 | 0.013664 |
| $X_1X_3$ | 1 | 1.1503 | 1.1503 | 0.54105 | 0.47334 |
| $X_1X_4$ | 1 | 0.079806 | 0.079806 | 4.2372E-005 | 0.99489 |
| $X_2X_3$ | 1 | 6.2500E-006 | 6.2500E-006 | 4.9271 | 0.042274 |
| $X_2X_4$ | 1 | 0.72676 | 0.72676 | 0.0071609 | 0.93368 |
| $X_3X_4$ | 1 | 0.0010563 | 0.0010563 | 8.1761 | 0.011937 |
| $X_1^2$ | 1 | 1.2060 | 1.2060 | 0.24016 | 0.63118 |
| $X_2^2$ | 1 | 0.035424 | 0.035424 | 2.0379 | 0.17390 |
| $X_3^2$ | 1 | 0.30060 | 0.30060 | 3.4047 | 0.084845 |
| $X_4^2$ | 1 | 0.50220 | 0.50220 | | |
| Residual | 15 | 2.2125 | 0.14750 | 0.23715 | 0.97465 |
| Lack of fit | 10 | 0.71181 | 0.071181 | | |
| Pure error | 5 | 1.5007 | 0.30015 | | |
| Cor. total | 29 | 27.144 | | | |

surface methodology was exercised to design the experiments and quadratic model was utilized for the prediction of the variables. With the help of CCD of RSM, the impacts of process variables including dye concentration, pH, adsorbent mass and contact time on adsorption of propyl paraben dye came under scrutiny. Under the conditions of pH of 4.0, propyl paraben dye concentration equal to 12 mg $L^{-1}$, adsorbent mass of 0.027 and sonication time of 3.0 min, the adsorption of propyl paraben dye onto titanium dioxide nanoparticles loaded on activated carbon was almost 99.8%. The experimental removal efficiency of titanium dioxide nanoparticles loaded on activated carbon got to $R^2 = 0.999$ for propyl paraben dye at optimal adsorption conditions. The excellent contribution of titanium dioxide nanoparticles loaded on activated carbon in deleting propyl paraben dye was confirmed when the lowest errors were obtained in no time. Equilibrium adsorption revealed that the system followed the Langmuir model. The highest adsorption capacity value of propyl paraben dye with titanium dioxide nanoparticles loaded on activated carbon was observed to be 120 mg $g^{-1}$. The kinetic studies brought to light that propyl paraben dye deletion followed pseudo-second-order rate equation.

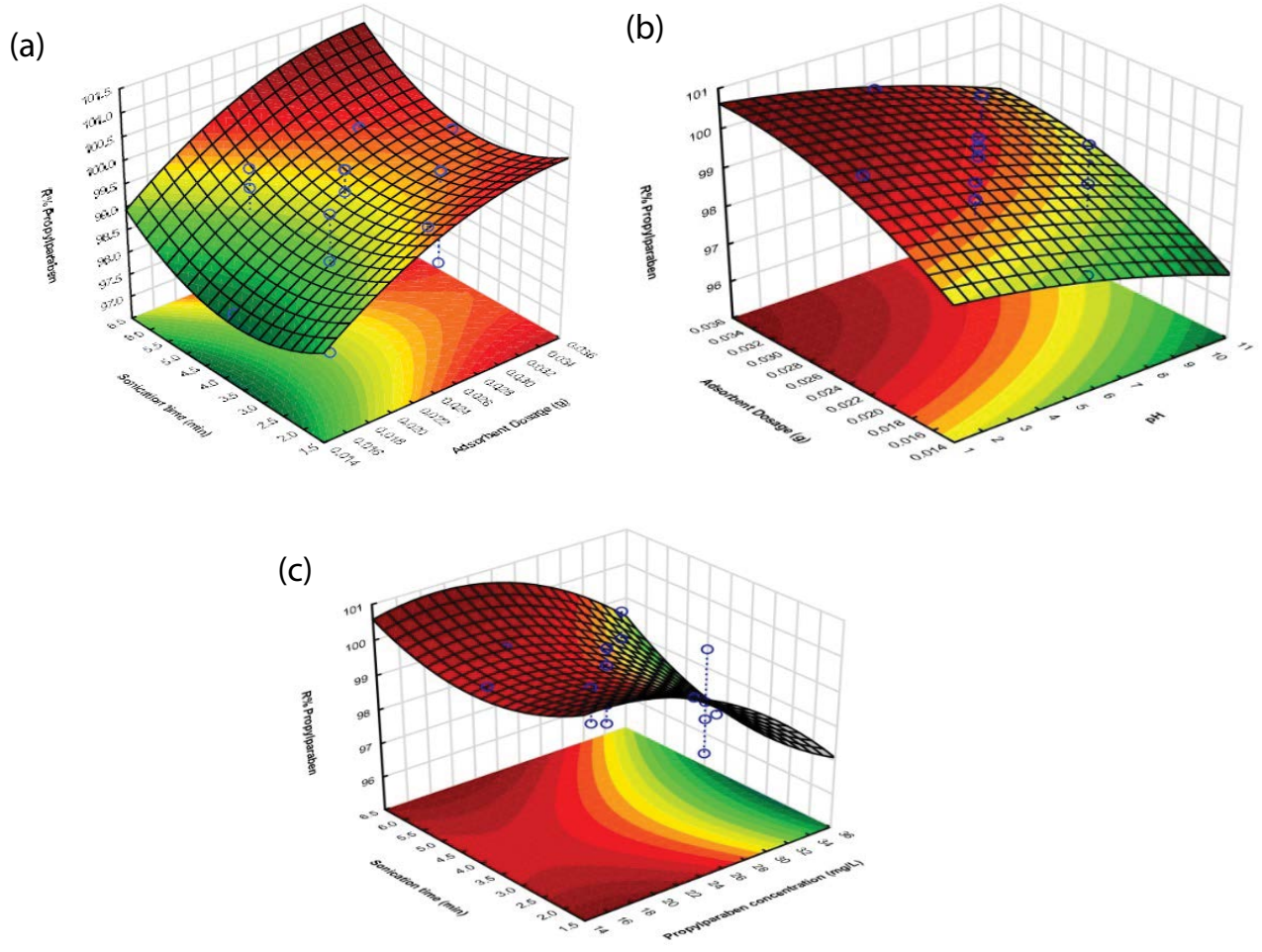


Fig. 4. Response surfaces for the CCD: (a) sonication time – adsorbent dosage, (b) adsorbent dosage – pH, and (c) sonication time – propyl paraben concentration.

Table 4
Various isotherm constants and their correlation coefficients calculated for the adsorption of propyl paraben onto $TiO_2$ NPs–AC

| Isotherm | Equation | Parameters | Value of parameters for propyl paraben |
|---|---|---|---|
| Langmuir | $q_e = q_m bC_e/(1 + bC_e)$ | $Q_m$ (mg g$^{-1}$) | 120 |
| | | $K_a$ (L mg$^{-1}$) | 0.240 |
| | | $R^2$ | 0.999 |
| Freundlich | $\ln q_e = \ln K_F + (1/n) \ln C_e$ | $1/n$ | 0.639 |
| | | $K_F$ (L mg$^{-1}$) | 4.95 |
| | | $R^2$ | 0.98 |
| Temkin | $q_e = B_1 \ln K_T + B_1 \ln C_e$ | $B_1$ | 30.28 |
| | | $K_T$ (L mg$^{-1}$) | 5.39 |
| | | $R^2$ | 0.978 |
| Dubinin–Radushkevich (DR) | $\ln q_e = \ln Q_s - B\varepsilon^2$ | $Q_s$ (mg g$^{-1}$) | 70.19 |
| | | $B \times 10^{-7}$ | –1 |
| | | $E$ (kJ mol$^{-1}$) | 2,272.72 |
| | | $R^2$ | 0.973 |

Table 5
Kinetic parameters for the adsorption of propyl paraben onto $TiO_2$ NPs–AC

| Model | Parameters | Value for propyl paraben |
|---|---|---|
| Pseudo-first-order kinetics | $k_1$ ($min^{-1}$) | 0.677 |
| | $q_e$ (calc) (mg $g^{-1}$) | 9.183 |
| | $R^2$ | 0.972 |
| Pseudo-second-order kinetics | $k_2$ ($min^{-1}$) | 0.124 |
| | $q_e$ (calc) (mg $g^{-1}$) | 45.45 |
| | $R^2$ | 0.999 |
| Intraparticle diffusion | $K_{diff}$ (mg $g^{-1}$ $min^{-1/2}$) | 3.72 |
| | $C$ (mg $g^{-1}$) | 35.07 |
| | $R^2$ | 0.974 |
| Elovich | $\beta$ (g $mg^{-1}$) | 0.375 |
| | $\alpha$ (mg $g^{-1}$ $min^{-1}$) | 65 |
| | $R^2$ | 0.972 |

Furthermore, desorption studies corroborated the possibility of recycling the adsorbent. With reference to the results of the linear regression-based analysis, it was reported that a satisfactory adsorbing performance onto titanium dioxide nanoparticles loaded on activated carbon was predictable from the empirical models with significant determination coefficients of $R^2 = 0.998$. In addition, the fact that the recommended equations could conveniently be utilized for the adsorption of propyl paraben dye from aqueous solutions was guaranteed by the statistical outcomes. Further considerations on the applicability of this adsorbent for the deletion of other materials have been highly recommended. Titanium dioxide nanoparticles loaded on activated carbon when juxtaposed against other adsorbents showed better performance in deleting propyl paraben dye from aqueous medium.

## Acknowledgment

The authors express their appreciation to the Science and Research Branch Islamic Azad University, Tehran, Iran, for financial support of this work.

## References

[1] D. Gryglik, M. Lach, J.S. Miller, The aqueous photosensitized degradation of butylparaben, Photochem. Photobiol. Sci., 8 (2009) 549–555.
[2] A. Prichodko, K. Jonusaite, V. Vickackaite, Hollow fibre liquid phase microextraction of parabens, Cent. Eur. J. Chem., 7 (2009) 285–290.
[3] D. Błedzka, D. Gryglik, J.S. Miller, Photodegradation of butylparaben in aqueous solutions by 254 nm irradiation, J. Photochem. Photobiol. A, 203 (2009) 131–136.
[4] J. Regueiro, E. Becerril, C. Garcia-Jares, M. Llompart, Trace analysis of parabens, triclosan and related chlorophenols in water by headspace solid-phase microextraction with in situ derivatization and gas chromatography tandem mass spectrometry, J. Chromatogr. A, 1216 (2009) 4693–4702.
[5] I. Gonzalez-Marino, J. Benito Quintana, I. Rodriguez, R. Cela, Simultaneous determination of parabens, triclosan and triclocarban in water by liquid chromatography/electrospray ionisation tandem mass spectrometry, Rapid Commun. Mass Spectrom., 23 (2009) 1756–1766.
[6] M. Chiara Pietrogrande, G. Basaglia, GC-MS analytical methods for the determination of personal-care products in water matrices, Trends Anal. Chem., 26 (2007) 1086–1094.
[7] P. Canosa, I. Rodriguez, E. Rubi, N. Negreira, R. Cela, Formation of halogenated by-products of parabens in chlorinated water, Anal. Chim. Acta, 575 (2006) 106–113.
[8] C. Zwiener, S.D. Richardson, Analysis of disinfection by-products in drinking water by LCMS and a related MS techniques, Trends Anal. Chem., 24 (2005) 613–621.
[9] K.S. Tay, N. Rahman, Kinetic studies of the degradation of parabens in aqueous solution by ozone oxidation, Environ. Chem. Lett., 7 (2009) 229–239.
[10] L. Nunez, J.L. Tadeo, A.I. Garcia-Valcarcel, E. Turiel, Determination of parabens in environmental solid samples by ultrasonic-assisted extraction and liquid chromatography with triple quadrupole mass spectrometry, J. Chromatogr. A, 1214 (2008) 178–182.
[11] A. Asfaram, M. Ghaedi, S. Hajati, A. Goudarzi, Synthesis of magnetic gamma-$Fe_2O_3$-based nanomaterial for ultrasonic assisted dyes adsorption: Modeling and optimization, Ultrason. Sonochem., 32 (2016) 418–431.
[12] E.C. Bernardo, T. Fukuta, T. Fujita, E.P. Ona, Y. Kojima, H. Matsuda, Enhancement of saccharin removal from aqueous solution by activated carbon adsorption with ultrasonic treatment, Ultrason. Sonochem., 13 (2006) 13–18.
[13] K. Kiani, S. Bagheri, N. Karachi, E. Alipanahpour Dil, Adsorption of purpurin dye from industrial wastewater using Mn-doped $Fe_2O_4$ nanoparticles loaded on activated carbon, Desal. Water Treat., 59 (2019) 1–8.
[14] A. Asfaram, M. Ghaedi, F. Yousefi, M. Dastkhoon, Experimental design and modeling of ultrasound assisted simultaneous adsorption of cationic dyes onto ZnS:Mn-NPs-AC from binary mixture, Ultrason. Sonochem., 33 (2016) 77–89.
[15] O. Acisli, A. Khataee, S. Karaca, M. Sheydaei, Modification of nanosized natural montmorillonite for ultrasound enhanced adsorption of Acid Red 17, Ultrason. Sonochem., 31 (2016) 116–121.
[16] M. Breitbach, D. Bathen, Influence of ultrasound on adsorption processes, Ultrason. Sonochem., 8 (2001) 277–283.
[17] M.H. Entezari, Z.S. Al-Hoseini, N. Ashraf, Fast and efficient removal of Reactive Black 5 from aqueous solution by a combined method of ultrasound and sorption process, Ultrason. Sonochem., 15 (2008) 433–437.
[18] H. Gupta, P.R. Gogate, Intensified removal of copper from waste water using activated watermelon based biosorbent in the presence of ultrasound, Ultrason. Sonochem., 30 (2016) 113–122.
[19] M. Jamshidi, M. Ghaedi, K. Dashtian, S. Hajati, A.A. Bazrafshan, Sonochemical assisted hydrothermal synthesis of ZnO:Cr nanoparticles loaded activated carbon for simultaneous ultrasound-assisted adsorption of ternary toxic organic dye: derivative spectrophotometric, optimization, kinetic and isotherm study, Ultrason. Sonochem., 32 (2016) 119–131.

[20] A. Mittal, D. Kaur, J. Mittal, Batch and bulk removal of a triarylmethane dye, Fast Green FCF, from wastewater by adsorption over waste materials, J. Hazard. Mater., 163 (2009) 568–577.
[21] G. Kiani, M.O. Dostalia, A. Rostami, A.R. Khataee, Adsorption studies on the removal of Malachite Green from aqueous solutions onto halloysite nanotubes, Appl. Clay Sci., 54 (2011) 34–39.
[22] A. Asfaram, M. Ghaedi, S. Agarwal, I. Tyagi, V. Kumar Gupta, Removal of basic dye Auramine-O by ZnS:Cu nanoparticles loaded on activated carbon: optimization of parameters using response surface methodology with central composite design, RSC Adv., 5 (2015) 18438–18450.
[23] P. Atheba, N. Guadi, B. Allou, P. Drogui, A. Trokourey, Adsorption kinetics and thermodynamics study of butylparaben on activated carbon coconut based, J. Encapsul. Adsorpt. Sci., 8 (2018) 39–57.
[24] A.R. Bagheri, M. Ghaedi, S. Hajati, A.M. Ghaedi, A. Goudarzi, A. Asfaram, Random forest model for the ultrasonic-assisted removal of chrysoidine G by copper sulfide nanoparticles loaded on activated carbon; response surface methodology approach, RSC Adv., 5 (2015) 59335–59343.
[25] R. Al Dwairi, A. Al-Rawajfeh, Bioavailability of heavy metals in soil amended with wastewater sludge, J. Univ. Chem. Technol. Metall., 47 (2012) 69–78.
[26] A. Naghizadeh, K. Gholami, Bentonite and montmorillonite nanoparticles effectiveness in removal of fluoride from water solutions, J. Water Health, 15 (2017) 555–565.
[27] A.R. Parvizi, S. Bagheri, N. Karachi, L. Niknam, Preparation and characterization of titanium dioxide nanoparticles for the removal of Disulfine Blue and Methyl Orange: spectrophotometric detection and optimization, Orient. J. Chem., 32 (2017) 549–565.
[28] S. Hajati, M. Ghaedi, B. Barazesh, F. Karimi, R. Sahraei, A. Daneshfar, A. Asghari, Application of high order derivative spectrophotometry to resolve the spectra overlap between BG and MB for the simultaneous determination of them: ruthenium nanoparticle loaded activated carbon as adsorbent, J. Ind. Eng. Chem., 20 (2014) 2421–2427.
[29] Y. Liu, G. Cui, C. Luo, L. Zhang, Y. Guo, S. Yan, Synthesis, characterization and application of amino-functionalized multiwalled carbon nanotubes for effective fast removal of methyl orange from aqueous solution, RSC Adv., 4 (2014) 55162–55172.
[30] A. Naghizadeh, M. Kamranifar, Montmorillonite nanoparticles in removal of textile dyes from aqueous solutions: study of kinetics and thermodynamics, Iran. J. Chem. Chem. Eng., 36 (2017) 127–137.
[31] A. Asfaram, M. Ghaedi, A. Goudarzi, M. Rajabi, Response surface methodology approach for optimization of simultaneous dye and metal ion ultrasound-assisted adsorption onto Mn doped $Fe_3O_4$-NPs loaded on AC: kinetic and isothermal studies, Dalton Trans., 44 (2015) 14707–14723.
[32] A. Asfaram, M. Ghaedi, S. Hajati, A. Goudarzi, A.A. Bazrafshan, Simultaneous ultrasound-assisted ternary adsorption of dyes onto copper-doped zinc sulfide nanoparticles loaded on activated carbon: optimization by response surface methodology, Spectrochim. Acta Part A, 145 (2015) 203–212.
[33] M. Dastkhoon, M. Ghaedi, A. Asfaram, M.H. Ahmadi Azqhandi, M.K. Purkait, Simultaneous removal of dyes onto nanowires adsorbent use of ultrasound assisted adsorption to clean waste water: chemometrics for modeling and optimization, multicomponent adsorption and kinetic study, Chem. Eng. Res. Des., 124 (2017) 222–237.
[34] M. Ghaedi, F. Karimi, B. Barazesh, R. Sahraei, A. Daneshfar, Removal of reactive orange 12 from aqueous solutions by adsorption on tin sulfide nanoparticle loaded on activated carbon, J. Ind. Eng. Chem., 19 (2013) 756–763.
[35] S. Bagheri, H. Aghaei, M. Ghaedi, A. Asfaram, M. Monajemi, A.A. Bazrafshan, Synthesis of nanocomposites of iron oxide/gold ($Fe_3O_4$/Au) loaded on activated carbon and their application in water treatment by using sonochemistry: optimization study, Ultrason. Sonochem., 41 (2018) 279–287.
[36] A. Mohammadi, A. Aliakbarzadeh Karimi, Methylene Blue removal using surface-modified $TiO_2$ nanoparticles: a comparative study on adsorption and photocatalytic degradation, J. Water Environ. Nanotechnol., 2 (2017) 118–128.
[37] M. Dinari, A. Haghighi, Surface modification of $TiO_2$ nanoparticle by three dimensional silane coupling agent and preparation of polyamide/modified-$TiO_2$ nanocomposites for removal of Cr(VI) from aqueous solutions, Prog. Org. Coat., 110 (2017) 24–34.
[38] M. Toor, B. Jin, Adsorption characteristics, isotherm, kinetics, and diffusion of modified natural bentonite for removing Diazo Dye, Chem. Eng. J., 187 (2012) 79–88.
[39] E.A. Dil, M. Ghaedi, A. Ghaedi, A. Asfaram, M. Jamshidi, M.K. Purkait, Application of artificial neural network and response surface methodology for the removal of crystal violet by zinc oxide nanorods loaded on activate carbon: kinetics and equilibrium study, J. Taiwan Inst. Chem. Eng., 59 (2016) 210–220.
[40] M. Ghaedi, A. Ansari, P. Assefi Nejad, A. Ghaedi, A. Vafaei, M.H. Habibi, Artificial neural network and bees algorithm for removal of eosin B using cobalt oxide nanoparticle-activated carbon: isotherm and kinetics study, Environ. Prog. Sustain. Energy, 34 (2015) 155–168.
[41] S. Bagheri, H. Aghaei, M. Ghaedi, M. Monajjemi, K. Zare, Novel Au–$Fe_3O_4$ NPs loaded on activated carbon as a green and high efficient adsorbent for removal of dyes from aqueous solutions: application of ultrasound wave and optimization, Eurasian J. Anal. Chem., 13 (2018) 1–10.